Exploring the impact of Bi_2O_3 addition on the thermal properties and crystallization behavior of lead borosilicate glasses

Yu. S. Hordieiev*, A. V. Zaichuk
Ukrainian State University of Chemical Technology, 8 Gagarin Avenue, Dnipro, 49005, Ukraine

Novel heavy-metal oxide glasses with different compositions, specifically (80-x)PbO–xBi_2O_3–10B_2O_3–10SiO_2, where x ranges from 0 to 60 mol%, were synthesized using a conventional melt-quenching technique. The amorphous nature of these glasses was confirmed through X-ray diffraction analysis. Additionally, infrared spectra were obtained for the prepared samples to explore their structural characteristics. Differential thermal analysis was performed to investigate the characteristic temperatures of the glasses, including the glass transition temperature, melting temperature, onset crystallization temperature, and peak crystallization temperature. The addition of Bi_2O_3 shifts the characteristic temperatures to higher values and affects the crystallization process and phases formed. Parameters like ΔT, K_H, and K_{SP} are used to evaluate and quantify glass stability. Dilatometric measurements demonstrated that substituting PbO with Bi_2O_3 in the glass composition resulted in an increase in glass transition temperature and dilatometric softening temperature, as well as a decrease in the coefficient of thermal expansion. Furthermore, we determined the density and calculated the molar volume of the samples. These findings deepen our understanding of the thermal behavior, glass stability, and structure-property relationships in lead borosilicate glasses with Bi_2O_3, facilitating the development and customization of glass compositions with desired thermal and physical characteristics for specific applications.

(Received June 23, 2023; Accepted August 30, 2023)

Keywords: Heavy-metal oxide glasses, Thermal expansion, Glass structure, Thermal stability, Crystallization

1. Introduction

Lead borosilicate glasses have garnered significant attention due to their exceptional properties, rendering them highly versatile for a wide range of applications [1–3]. The combination of lead oxide, boron oxide, and silicon dioxide in these glasses results in a unique combination of characteristics, including a low melting point [4], high refractive index [5], low dispersion [6], excellent chemical durability [7], good electrical resistivity [8], and effective radiation shielding capabilities [9].

One notable area where lead borosilicate glasses exhibit immense promise is optics [10]. Their high refractive index makes them ideal for fabricating lenses, prisms, and other optical components. Consequently, they find extensive usage in high-power lasers, telescopes, and various optical instruments, where their optical properties contribute to superior performance [11]. Lead borosilicate glasses also find applications in the electronics industry. Their low melting points make them advantageous for use as solder glasses, protective coatings, and sealing materials in semiconductor devices and integrated circuits [12–14]. The low melting temperature prevents oxidation and deformation of metallic parts during the soldering process, ensuring the integrity of electronic components [15]. Another important area of study for lead borosilicate glasses is their potential use in nuclear waste disposal. These glasses possess high densities and excellent radiation shielding properties, making them attractive for immobilizing high-level radioactive waste [16–18]. As a matrix material, lead borosilicate glasses can effectively encapsulate

* Corresponding author: yuriihordieiev@gmail.com
https://doi.org/10.15251/JOR.2023.194.471

radioactive elements, preventing their release and providing long-term stability. The combination of lead oxide and boron oxide in these glasses contributes to their ability to trap and contain radioactive species. Overall, the extensive study of lead borosilicate glasses stems from their versatile nature and the wide range of properties they offer.

Lead borosilicate glasses, despite their advantageous properties, are not without limitations. One significant challenge associated with these glasses is their proneness to devitrification [4], which refers to the process of crystallization or transformation into a crystalline material over time, particularly when exposed to higher temperatures. Devitrification can have adverse effects, leading to the loss of desirable properties and an increase in the glass's brittleness. However, researchers are actively working toward addressing this challenge by deepening their understanding of the intricate relationship between the composition, structure, and thermal properties of lead borosilicate glasses. This knowledge enables them to develop effective strategies that can mitigate devitrification and tailor glass formulations to specific applications while preserving the glass's unique properties [4]. By carefully adjusting the ratios of lead oxide, boron oxide, and silicon dioxide or by incorporating additional oxides, it becomes possible to stabilize the glass structure and enhance its thermal stability [19–22]. Bismuth oxide (Bi_2O_3) is a promising replacement for PbO in lead-borosilicate glasses due to its similar chemical and physical properties [23]. The addition of Bi_2O_3 to lead borosilicate glasses can result in changes in their thermal properties, such as the glass transition temperature, coefficient of thermal expansion (CTE) and thermal stability. One of the reasons for these changes is the ability of Bi_2O_3 to form stronger chemical bonds with the glass network compared to PbO [24]. Furthermore, the addition of Bi_2O_3 can also affect the crystallization behavior of the glass. The addition of Bi_2O_3 can alter the crystal phases that form upon crystallization and their morphology, which can affect the properties of the glass. In summary, replacing PbO with Bi_2O_3 in lead borosilicate glasses can significantly affect their thermal properties and crystallization behavior. However, it is important to carefully consider the composition and amount of Bi_2O_3 added, as excessive amounts may lead to detrimental effects on the glass structure and properties.

Hence, the objective of this research was to examine how the incorporation of Bi_2O_3 affects the crystallization behavior and thermal properties of 80PbO–10B2O3–10SiO glass using X-ray diffraction (XRD), scanning electron microscopy (SEM), Fourier-transform infrared spectroscopy (FTIR), differential thermal analysis (DTA), and dilatometry technique.

2. Materials and methods

Lead-bismuth borosilicate glass compositions with their labels are listed in Table 1. Glasses in the molar composition of $(80\text{-}x)PbO–xBi_2O_3–10B_2O_3–10SiO_2$ (x = 0, 10, 20, 30, 40, 50 and 60 mol %) were obtained by a conventional melt-quenching technique using Pb_3O_4 (99.5%, Colorobbia), Bi_2O_3 (99.9%, Sigma–Aldrich), H_3BO_3 (99.9%, Eti Mine Works) and SiO_2 (99.9%, Polar Quartz) as raw materials. The corresponding components were thoroughly mixed with an agate mortar and melted in a 50 mL platinum crucible at 950–1000°C for 30 minutes using an electric furnace with silicon carbide (SiC) heaters. The resulting molten glass was then poured quickly into a preheated stainless-steel mold. The glass samples were then subjected to annealing in a muffle furnace at a temperature of 300°C for 5 hours and allowed to cool gradually to room temperature to prevent any internal stress.

Table 1. Chemical composition (mol %) of the investigated glasses.

Sample name	Glass composition			
	PbO	Bi_2O_3	B_2O_3	SiO_2
80Pb	80	0	10	10
70Pb10Bi	70	10	10	10
60Pb20Bi	60	20	10	10
50Pb30Bi	50	30	10	10
40Pb40Bi	40	40	10	10
30Pb50Bi	30	50	10	10
20Pb60Bi	20	60	10	10

In order to prepare the glass sample for differential thermal analysis, it was ground into a fine powder using an agate mortar and pestle and then passed through a series of standard sieves. The portion of the powder that passed through a 270 mesh (53 μm) sieve was selected for analysis. The DTA analysis was carried out using a Derivatograf Q-1500D. The glass transition temperature (T_g), onset crystallization temperature (T_x), peak crystallization temperature (T_c), and melting temperature (T_m) were measured by heating the glass sample at a constant rate of 5°C/min from room temperature to 1000°C in an air atmosphere. High-purity alumina powder was used as the reference substance, and the temperature error was ±5°C. The glass transition temperature (T_g) was determined as the onset of the first endothermic peak on the DTA curves [19]. To identify the crystalline phases linked to the exothermic peaks in the DTA curves, the glass powder was heat-treated in the air at the crystallization temperature (T_c) for 5 hours. The crystalline phases that formed during the heat treatment process were identified using a DRON-3M X-ray diffractometer that utilized Co-Kα radiation to scan the $10 < 2\Theta < 90$ range. The microstructure of the crystalline phases developed in the glass-ceramic samples after heat treatment was examined by scanning electron microscopy (FESEM, MIRA3 TESCAN) operating at 10 kV.

The FTIR transmitting spectra were obtained using the Thermo Nicolet Avatar 370 FTIR Spectrometer in the 1600–400 cm^{-1} range with a resolution of 2 cm^{-1}. The KBr pellet technique was used, wherein each sample (2 mg of glass powder) was mixed with 200 mg of KBr in an agate mortar and then pressed into pellets with a diameter of 13 mm [25]. The spectrum for each sample was the average of 32 scans and was normalized to the spectrum of the blank KBr pellet [25].

The glass samples were subjected to measurements of their dilatometric softening point (T_d), glass transition temperature (T_g), and coefficient of thermal expansion (CTE) using a dilatometer 1300 L (Italy), which had a heating rate of 3°C/min. The CTE value was determined within the range of 20 to 200°C (as shown in Fig. 1). The dilatometry analysis results are presented in Table 2. Additionally, the density of the glass samples was measured at room temperature using distilled water as the immersion liquid and a digital balance with 10^{-4} g sensitivity.

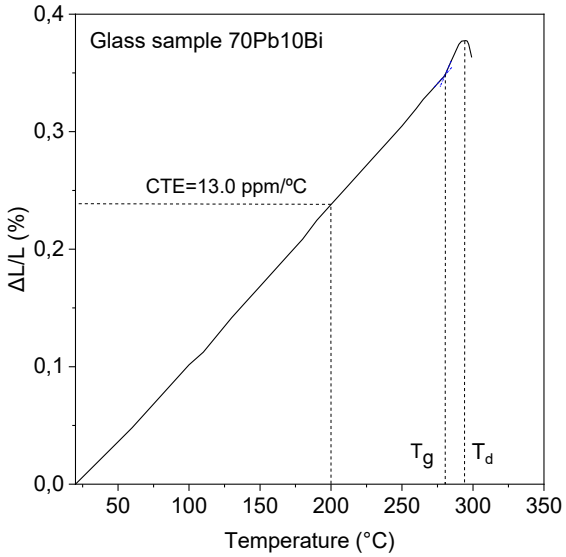

Fig. 1. Dilatometry curve of 70Pb10Bi sample.

3. Results and discussion

XRD analysis results (Fig. 2) indicate that all the prepared glass samples in the mentioned compositions are amorphous, as demonstrated by the absence of crystallization peaks and the presence of a broad halo pattern around 2θ = 33°, which is characteristic of amorphous materials. Amorphous materials lack the long-range atomic arrangement and periodicity observed in crystalline materials and instead display a disordered atomic structure, which is reflected in the broad halo pattern observed in the XRD analysis.

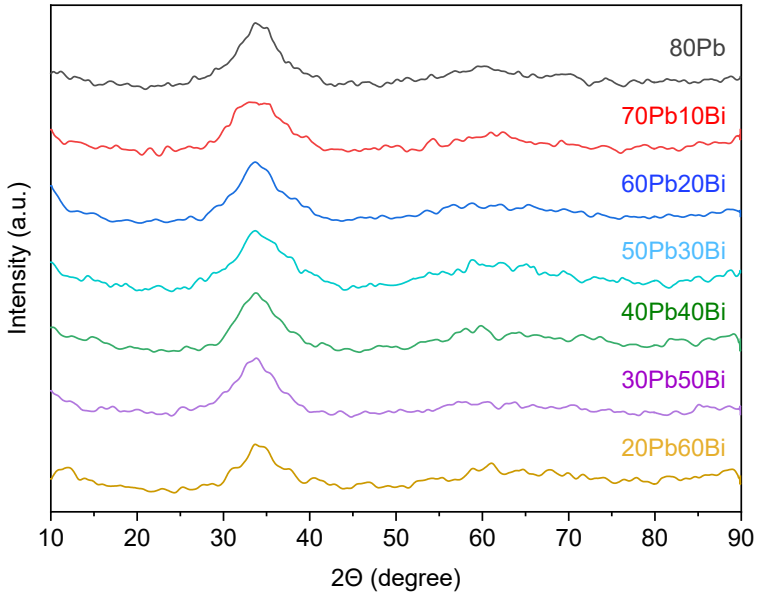

Fig. 2. X-ray powder diffraction patterns of the investigated glasses.

Utilizing Fourier-transform infrared (FTIR) spectroscopy can greatly enhance our understanding of the local structure, properties, and behavior of glasses. The infrared transmission

spectra of the prepared glass samples were examined within the wavenumber range of 400–1600 cm^{-1}. Figure 3 shows the FTIR spectra for all samples. Existing literature [3, 11, 26–30] on lead borosilicate and bismuth borosilicate glasses was consulted to interpret the spectra and identify absorption bands. The FTIR spectra of the prepared samples exhibit bands typical of borosilicate glasses, specifically around 1240 cm^{-1}, 1150 cm^{-1}, 870 cm^{-1} and 705 cm^{-1}. The absorption band at approximately 1240 cm^{-1} is typically attributed to the B–O stretching vibrations of the BO_3 units present in boroxol rings [3, 11, 26]. The infrared absorption band at about 1150 cm^{-1} is assigned to the absorption vibration of BO_4 units [11, 27, 28]. This band is due to the stretching vibration of the oxygen atoms in the BO_4 units. The fact that both bands have an equal intensity indicates that the two types of units are present in equal proportions. The symmetric stretching of Si–O bonds in SiO_4 tetrahedra is responsible for the absorption peak at 870 cm^{-1} [3, 11]. The absorption band at 705 cm^{-1} is caused by the bending vibrations of the B–O–B bonds in BO_3 triangles [3, 11, 26]. The decrease in the peak area at 705 cm^{-1} with increasing Bi_2O_3 content indicates that the concentration of BO_3 units is decreasing, while the increase in the band intensity at 1150 cm^{-1} indicates that the concentration of BO_4 units is increasing. This suggests that the addition of Bi_2O_3 to borate glasses leads to a transformation of BO_3 units into BO_4 units. The overall effect of increasing Bi_2O_3 content is to increase the connectivity of the boron network and make the glass more rigid. Additionally, the study showed that substituting PbO with Bi_2O_3 results in the suppression of the absorption band at 615 cm^{-1}, which originates from the bending vibrations of the B–O–Pb bonds within the glass network [29, 30]. Simultaneously, a new band emerges at approximately 560 cm^{-1}, indicating the presence of symmetrical stretching vibrations of Bi–O–Bi bonds in the BiO_6 octahedral unit [27, 31]. The distinct broad band observed at approximately 460 cm^{-1} on the spectra of all glass samples is ascribed to the bending vibration of the Si–O–Si bond in SiO_4 tetrahedra and the symmetric bending vibration of the Pb–O bond in PbO_4 tetrahedra [3, 27].

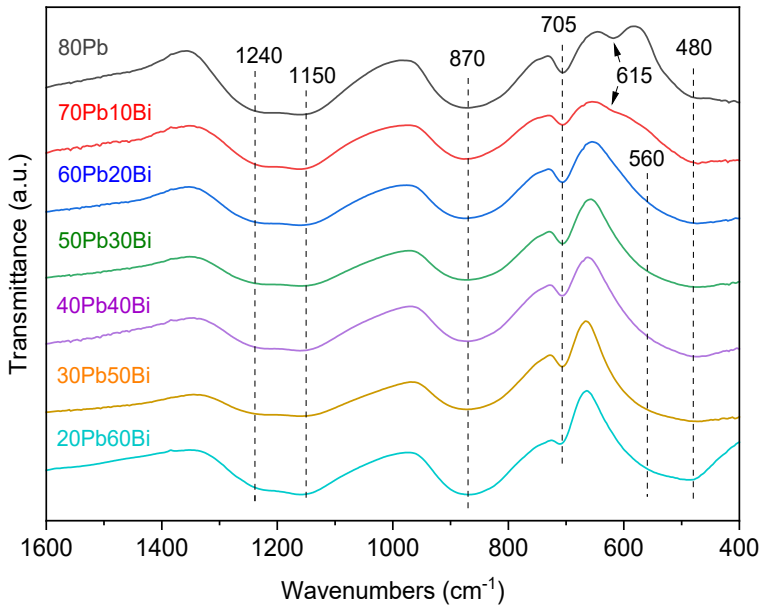

Fig. 3. FTIR spectra for (80-x)PbO–xBi_2O_3–10B_2O_3–10SiO_2 glasses with x = 0–60 mol%.

Differential thermal analysis (DTA) was used to thoroughly analyze the thermal behavior of lead-bismuth borosilicate glasses. The DTA curves in Fig. 4 illustrate the thermal behavior of the 70Pb10Bi glass sample at different heating rates.

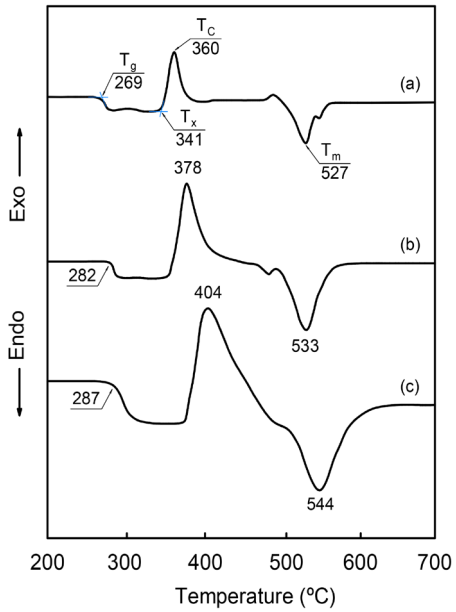

Fig. 4. DTA results of 70Pb10Bi sample at different heating rates: (a) 2.5 °C/min, (b) 5 °C/min and (c) 10 °C/min.

The results indicate that, similar to other glassy systems [32, 33], the glass transition temperature (T_g) and other characteristic temperatures of the glasses increase with higher heating rates. This phenomenon has been previously explained in the literature [32]. The reasoning behind this phenomenon is that higher heating rates provide greater heat per unit time. The glass transition occurs when the relaxation time approaches the isothermal holding time. At higher heating rates, the relaxation time decreases and becomes comparable to the isothermal holding time, leading to the glass transition taking place. T_g is inversely proportional to the relaxation time, which, in turn, is inversely proportional to the heating rate. Therefore, as the heating rate increases, T_g also increases. This finding aligns with the observations made in this study and supports the notion established in the literature. The heating rate plays a significant role in the nucleation and crystallization processes of glass, affecting the concentration of nucleation sites, the crystallization temperature range, and the resulting crystallites' size. Lower heating rates provide more time for nucleation, resulting in a higher concentration of nucleation sites and a shift of the crystallization onset to lower temperatures, as indicated by the shift of T_c into the region of lower temperatures. The crystallization peak observed in DTA analysis becomes broader and more intense at higher heating rates, indicating shorter crystallization times and the formation of larger crystallites.

Fig. 5 presents DTA curves for all the investigated glasses but with a fixed heating rate of 5°C/min. These curves provide valuable information about the characteristic temperatures of the glasses, including T_g, T_m (melting temperature), T_x (onset crystallization temperature), and T_c (peak crystallization temperature) [34].

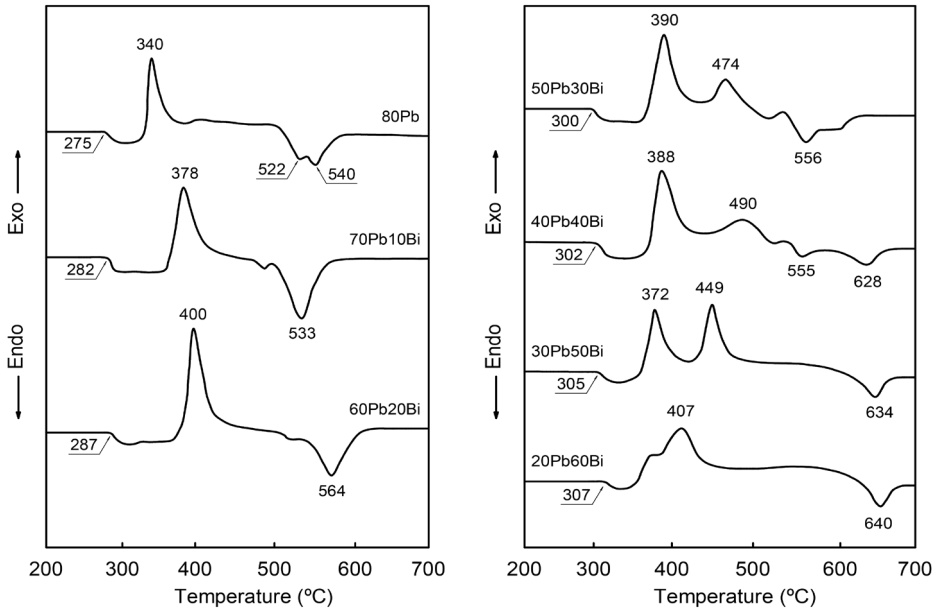

Fig. 5. DTA curves of investigated glasses using fine powders with a heating rate of 5 °C/min.

Figure 5 demonstrates that all the DTA scans displayed an endothermic transition within the temperature range of 270 to 310°C. This transition corresponds to the glass transition temperature (T_g) and provides confirmation that the investigated samples possess a glassy nature. Replacing PbO with Bi_2O_3 shifts all characteristic temperatures to higher values. Figure 5 shows that the number of exothermic peaks, which indicate crystallization reactions, varies with the change in composition. Glass samples containing 30–50 mol% Bi_2O_3 exhibit two distinct exothermic peaks in their DTA curves, indicating a complex crystallization process and the formation of two crystalline phases. On the other hand, only one exothermic peak is observed in the DTA curves of the other investigated glasses, suggesting the formation of a single crystalline phase. Selected samples were heat-treated at the peak crystallization temperatures to identify the resulting phases. The peak crystallization temperatures for the different compositions were: 340°C for 80Pb, 390°C for 70Pb10Bi, 390 and 474°C for 50Pb30Bi, and 407°C for 20Pb60Bi. The corresponding XRD patterns after heat treatment are shown in Fig. 6. XRD analysis revealed that 5-hour heat treatment at 340°C for the base glass (80Pb) resulted in the formation of a single crystalline phase, $Pb_4B_2O_7$ (PDF 00-003-576). For the glass with 10 mol% Bi_2O_3 (70Pb10Bi), the main crystalline phase formed after heat treatment at 390°C is Pb_3SiO_5 (PDF 00-029-0783). Notably, the addition of bismuth oxide to the lead borosilicate glass affects both the main crystalline phase and crystal morphology (Fig. 7). The 80Pb sample exhibits long needle-like crystals (0.5–2 μm) surrounded by an amorphous matrix, while the 70Pb10Bi sample displays larger rhombus-shaped crystals (1–5 μm). The XRD patterns of the 50Pb30Bi sample, after heat treatment, indicate the formation of two distinct phases: $Pb_4Bi_3B_7O_{19}$ (PDF 00-039-0570) and $Bi_{12}SiO_{20}$ (PDF 00-037-0485). Finally, in the case of the glass with 60 mol% Bi_2O_3, the only product of crystallization upon heat treatment was $Bi_{12}SiO_{20}$ (PDF 00-037-0485).

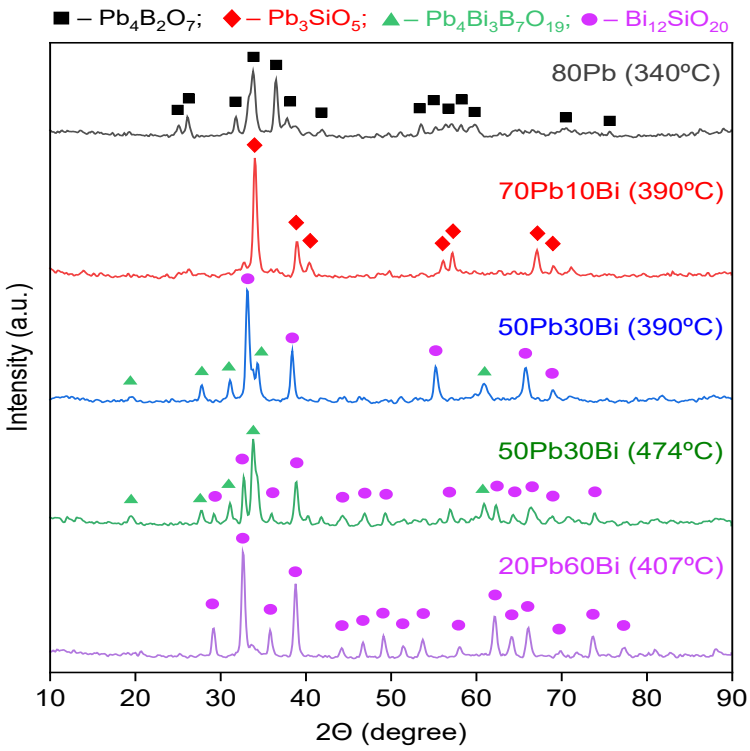

Fig. 6. X-ray diffraction patterns of glass powders heat treated at the crystallization temperature for 5 hours.

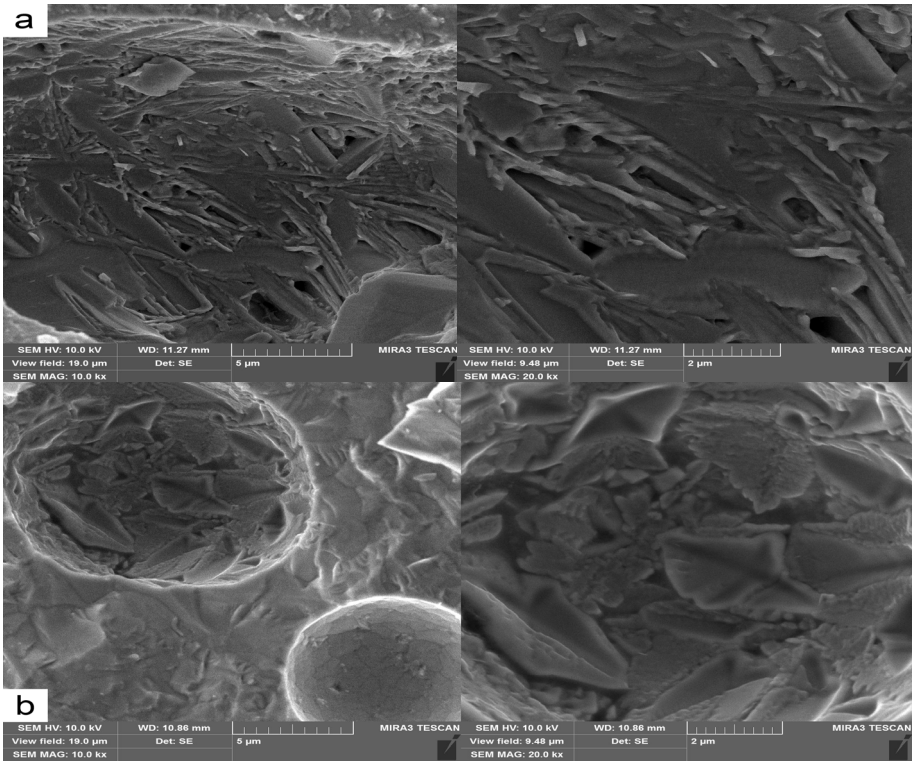

Fig. 7. SEM micrograph of the fractured surface of glass-ceramic samples derived from the 80Pb (a) and 70Pb10Bi (b) glasses after undergoing a 5-hour heat treatment.

Glass stability is a crucial characteristic that measures the ability of a glass material to maintain its amorphous structure when subjected to heating. Devitrification, which is the

crystallization of the glass upon heating, can significantly affect the properties and performance of the material. Therefore, assessing and understanding glass stability is essential for developing and applying glass materials in various industries. Various parameters have been proposed to evaluate and quantify glass stability, primarily based on characteristic temperatures associated with the glass transition, crystallization, and melting processes. These parameters provide valuable insights into the thermal behavior of glasses and their resistance to devitrification. Three notable examples of such parameters are the Dietzel criterion ($\Delta T = T_x - T_g$) [35], the Hruby criterion ($K_H = (T_c - T_g)/(T_m - T_c)$) [36], and the Saad and Poulain criterion ($K_{SP} = (T_c - T_x)\Delta T/T_g$) [37]. Higher values of these parameters correspond to greater thermal stability, indicating that the glass is less likely to undergo crystallization under heating conditions. From Table 2, it is noted that as the Bi_2O_3 content increases from 0 to 20 mol%, the values of ΔT, K_H, and K_{SP} also increase. This indicates that the addition of Bi_2O_3 enhances the glass stability within this range. A higher ΔT signifies a larger temperature window between the glass transition and crystallization, suggesting improved thermal stability. Similarly, higher K_H and K_{SP} values indicate slower crystallization kinetics, implying increased resistance to crystallization. However, when the amount of Bi_2O_3 exceeds the optimal range (20 mol% in this case), the glass structure becomes excessively modified. The excessive modification weakens the glass network, making it more prone to structural rearrangements and crystallization when exposed to elevated temperatures. Consequently, the parameters ΔT, K_H, and K_{SP} start to decrease, indicating a decrease in glass stability.

Table 2. Values of the characteristic temperatures (T_g, T_d, T_x, T_c, T_m), stability parameters (ΔT, K_{SP}, K_H), coefficient of thermal expansion (CTE), density (ρ) and molar volume (V_m) of the investigated glasses.

Sample name	ρ, g/cm^3	V_m, cm^3/g	Dilatometry			DTA				Stability parameters		
			T_g, °C	T_d, °C	CTE, ppm/°C	T_g, °C	T_x, °C	T_c, °C	T_m, °C	ΔT, °C	K_{SP}, °C	K_H
80Pb	7.49	25.57	270	290	13.1	275	323	340	522	48	2.97	0.36
70Pb10Bi	7.74	27.88	280	295	13	282	353	380	533	71	6.29	0.62
60Pb20Bi	7.82	30.70	285	300	12.8	287	370	400	564	83	8.68	0.69
50Pb30Bi	7.88	33.55	290	303	12.7	300	350	390	556	50	6.67	0.54
40Pb40Bi	7.94	36.35	295	305	12.6	302	340	388	628	38	6.04	0.36
30Pb50Bi	8.01	39.07	297	308	12.5	305	335	372	634	30	3.64	0.26
20Pb60Bi	8.07	41.79	303	315	12.4	307	330	407	640	23	5.77	0.43

In the realm of materials science and engineering, thermal expansion, glass transition temperature, and dilatometric softening temperature hold significant importance. These properties offer valuable insights into how glass behaves under different temperature conditions, aiding in determining its suitability for specific applications. A crucial factor influencing these properties is the oxide composition of the glass. Examining the results obtained from dilatometry shows that the equimolar substitution of PbO by Bi_2O_3 leads to notable changes. The glass transition temperature increases from 270 to 303°C, while the dilatometric softening point increases from 290 to 315°C. Conversely, the coefficient of thermal expansion decreases from 13.1 to 12.4 ppm/°C. These alterations can be attributed to substituting weaker Pb–O bonds (with a bond energy of 101 kJ/mol) with stronger Bi–O bonds (with a bond energy of 102.5 kJ/mol) [24]. Additionally, the density (7.49–8.07 g/cm^3) and molar volume (25.57–41.79 cm^3/mol) of the glasses increase as PbO is substituted with Bi_2O_3. This increase in density is primarily due to the relatively larger molar mass of Bi_2O_3 compared to PbO. Moreover, the larger ionic radius of the substituted Bi^{2+} ions causes an increase in the molar volume of the glass. These findings deepen our understanding of the structure-property relationships in glasses and enable the tailoring of glass compositions for specific applications based on the desired thermal and physical characteristics.

4. Conclusions

The thermal properties and crystallization behavior of lead-bismuth borosilicate glasses with varying compositions (80-x)PbO–xBi_2O_3–10B_2O_3–10SiO_2 (where x = 0–60 mol%) were extensively investigated using analytical techniques such as X-ray diffraction, scanning electron microscopy, Fourier-transform infrared spectroscopy, differential thermal analysis, and dilatometry. The X-ray diffraction patterns confirmed that the glasses exhibited an amorphous structure. Differential thermal analysis curves provided additional evidence of the glassy nature of the samples and offered insights into characteristic temperatures such as T_g, T_m, T_x, and T_c.

The addition of Bi_2O_3 to the lead borosilicate glass composition affects these characteristic temperatures, shifting them to higher values. Among the studied glass samples, the one with 20% Bi_2O_3 exhibited the highest values of ΔT, K_H, and K_{SP}, indicating its superior thermal stability compared to the other samples. The number of exothermic peaks in the DTA curves varied with the composition, indicating a complex crystallization process and the formation of multiple crystalline phases in some samples. Heat treatment at specific temperatures led to the formation of distinct crystalline phases, as determined by XRD analysis. Equimolar substitution of PbO with Bi_2O_3 increased the glass transition temperature, dilatometric softening temperature, density, and molar volume, while decreasing the coefficient of thermal expansion.

Acknowledgements

This work was partly supported by the Ministry of Education and Science of Ukraine.

References

[1] S. A. M. Issa, Y. B. Saddeek, H. O. Tekin, M. I. Sayyed, and K. S. Shaaban, Curr. Appl. Phys. **18**(6), 717 (2018); https://doi.org/10.1016/j.cap.2018.02.018
[2] O. Krupych, I. Martynyuk-Lototska, A. Say, V. Boyko, V. Goleus, Y. Hordieiev, and R. Vlokh, Ukr. J. Phys. Opt. **21**, 47 (2020); https://doi.org/10.3116/16091833/21/1/47/2020
[3] G. E. Rachkovskaya, G. B. Zakharevich, Glass and Ceramics volume **61**, 9 (2004); https://doi.org/10.1023/B:GLAC.0000026761.65840.58
[4] V. I. Goleus, Y. S. Hordieiev, A. V. Nosenko, Voprosy Khimii i Khimicheskoi Tekhnologii **4**, 92 (2018).
[5] B. V. Padlyak, I. I. Kindrat, A. Drzewiecki, V. I. Goleus, and Y. S. Hordieiev, J. Non Cryst. Solids **557**, 120631 (2021); https://doi.org/10.1016/j.jnoncrysol.2020.120631
[6] D. Singh, K. Singh, G. Singh, Manupriya, S. Mohan, M. Arora, G. Sharma, J. Phys.: Condens. Matter **20**, 075228 (2008); http://doi.org/10.1088/0953-8984/20/7/075228
[7] A. Khanna, A. Saini, B. Chen, F. Gonzalez, B. Ortiz, Phys. Chem. Glasses Eur. J. Glass Sci. Technol. Part B **55**(2), 65 (2014).
[8] G. El-Damrawi, E. Mansour, Physica B: Condensed Matter **364**(1-4), 190 (2005); http://doi.org/10.1016/j.physb.2005.04.012
[9] M. Humaid, J. Asad, A. Aboalatta, S. K. K. Shaat, H. Musleh, Kh. Ramadan, Y. Alajerami, N. Aldahoudi, Construction and Building Materials **375**, 130896 (2023); https://doi.org/10.1016/j.conbuildmat.2023.130896
[10] B. V. Padlyak, I. I. Kindrat, Y. O. Kulyk, S. I. Mudry, A. Drzewiecki, Y. S. Hordieiev, V. I. Goleus, and R. Lisiecki, Mater. Sci. Eng. B Solid State Mater. Adv. Technol. **278**, 115655 (2022); https://doi.org/10.1016/j.mseb.2022.115655
[11] M. S. Gaafar, S. Y. Marzouk, I. S. Mahmoud, Results in Physics **22**, 103944 (2021); https://doi.org/10.1016/j.rinp.2021.103944
[12] S. Fujino, C. Hwang, K. Morinaga, J. Am. Ceram. Soc. **87**, 10 (2004); https://doi.org/10.1111/j.1151-2916.2004.tb19937.x
[13] Yu. S. Hordieiev, A. V. Zaichuk, Chalcogenide Letters **19**(12), 891 (2022); https://doi.org/10.15251/CL.2022.1912.891

[14] N. M. Bobkova, S. A. Khot'ko, Glass and Ceramics **61**, 175 (2004); https://doi.org/10.1023/B:GLAC.0000043085.41234.be
[15] A. V. Nosenko, Y. S. Hordieiev, V. I. Goleus, Voprosy Khimii i Khimicheskoi Tekhnologii **1**, 87 (2018).
[16] P. B. Jahagirdar, P. K. Wattal, Waste Manag. **18**, 265 (1998); https://doi.org/10.1016/s0956-053x(98)00025-7
[17] C. Niu, C. Zhao, X. Zhou, K. Xu, J. Non Cryst. Solids. **603**, 122110 (2023); https://doi.org/10.1016/j.jnoncrysol.2022.122110
[18] D. Pletser, R.K. Chinnam, M. Kamoshida, W.E. Lee, MRS Adv. **1**(62), 4089 (2016); https://doi.org/10.1557/adv.2017.194
[19] Yu. S. Hordieiev, A. V. Zaichuk, MRS Advances **8**(5), 201 (2023); https://doi.org/10.1557/s43580-023-00511-7
[20] J. H. Jean, C. R. Chang, S. C. Lin, S. L. Yang, Mater. Chem. Phys. **43**, 31 (1996); https://doi.org/10.1016/0254-0584(95)01592-i
[21] E. V. Karasik, Yu. S. Hordieiev, Voprosy Khimii i Khimicheskoi Tekhnologii **6**, 69 (2020); https://doi.org/10.32434/0321-4095-2020-133-6-69-74
[22] H. H. Somaily, K. S. Shaaban, S. A. Makhlouf, H. Algarni, H. H. Hegazy, E. A. A. Wahab, E. R. Shaaban, J. Inorg. Organomet. Polym. Mater. **31**, 138 (2021); https://doi.org/10.1007/s10904-020-01650-2
[23] T. Maeder, Int. Mater. Rev. **58**, 3 (2013); https://doi.org/10.1179/1743280412y.0000000010
[24] V. Dimitrov, T. Komatsu, J. Univ. Chem. Technol. Metall. **45**, 219 (2010).
[25] Yu. S. Hordieiev, A. V. Zaichuk, J. Inorg. Organomet. Polym. Mater. **33**(2), 591 (2023); https://doi.org/10.1007/s10904-022-02526-3
[26] S. Gu, Z. Wang, S. Jiang, H. Lin, Ceram. Int. **40**, 7643 (2014); https://doi.org/10.1016/j.ceramint.2013.12.093
[27] M. A. Marzouk, S. M. Abo-Naf, H. A. Zayed, N. S. Hassan, Silicon **10**, 21 (2018); https://doi.org/10.1007/s12633-015-9342-3
[28] A. M. Al-Baradi, E. A. A. Wahab, K. S. Shaaban, Silicon **14**, 5277 (2022); https://doi.org/10.1007/s12633-021-01286-y
[29] S. Rada, M. Culea, M. Neumann, E. Culea, Chem. Phys. Lett. **460**, 196 (2008); https://doi.org/10.1016/j.cplett.2008.05.088
[30] E. Mansour, J. Non Cryst. Solids. **358**, 454 (2012); https://doi.org/10.1016/j.jnoncrysol.2011.10.037
[31] L. Xia, X. Ye, H. Ge, Y. Qiang, Q. Xiao, Q. Zhang, Z. Tong, Ceram. Int. **43**, 17005 (2017); https://doi.org/10.1016/j.ceramint.2017.09.109
[32] S. S. Danewalia, K. Singh, S. K. Arya, J. Non Cryst. Solids. **553**, 120471 (2021); https://doi.org/10.1016/j.jnoncrysol.2020.120471
[33] S. Pawaria, M. Bala, H. Duhan, N. Deopa, S. Dahiya, A. Ohlan, R. Punia, A.S. Maan, J. Therm. Anal. Calorim. **147**, 13099 (2022); https://doi.org/10.1007/s10973-022-11531-0
[34] Yu. S. Hordieiev, E. V. Karasik, A. V. Zaichuk, Silicon **15**, 1085 (2023); https://doi.org/10.1007/s12633-022-01745-0
[35] A. Dietzel, Glasstech Ber. **22**, 41 (1968).
[36] A. Hrubý, Czechoslov. J. Phys. **22**, 1187 (1972); https://doi.org/10.1007/bf01690134
[37] M. Saad, M. Poulain, Mater. Sci. For. **19–20**, 11 (1987); https://doi.org/10.4028/www.scientific.net/msf.19-20.11